

Surface-modified substrates for the Langmuir Blodgett deposition of
patterned ultra-thin and highly oriented collagen coatings

Karina Ambrock ^a, Bernd Grohe ^b and Silvia Mittler ^{a,*}

^a Department of Physics and Astronomy, University of Western Ontario, London, Ontario,
Canada N6A 3K7; Email: Karina.Ambrock@uni-muenster.de

^b Department of Chemical and Biochemical Engineering, University of Western Ontario,
London, ON, Canada N6A 5B9; Email: bgrohe@uwo.ca, ORCiDs: 0000-0001-6923-6538

^c Department of Physics and Astronomy, University of Western Ontario, London, Ontario,
Canada N6A 3K7; Email: smittler@uwo.ca, ORCiDs: 0000-0001-8998-1877

* Corresponding author: Silvia Mittler: Email: smittler@uwo.ca, Tel: +1 519-661-2111 ext.
88592, Fax: +1 519-661-2033, ORCiDs: 0000-0001-8998-1877

Abstract: As a pre-study for highly oriented collagen coatings on implants (with irregular surfaces and shapes), the Langmuir-Blodgett (LB) technology, a low-cost and straightforward approach, was pioneered. The effects of physicochemical (hydrophilic / hydrophobic) patterns and 3D-mechanical barriers present on substrate surfaces are studied in terms of the dynamics of collagen flow during LB film deposition and the formation of highly oriented coatings. Due to the large internal cohesion of collagen films only large 3D-obstacles deflect the flow of collagen and lead to film rupture, suggesting that objects (screw-threaded dental implants) with small topographic features should be easily and evenly coatable. Moreover, hydrophilic / hydrophobic / collagen patterned substrate surfaces were fabricated, by partly removing coated collagen. These substrates are outstanding for timely studies that need identical conditions but different surface properties side by side. Crystallization of barium oxalate was carried out as a proof-of-principle.

Keywords: Langmuir-Blodgett technology; collagen deposition; ultra-thin collagen coatings; highly oriented collagen; surface-modified substrates; hydrophobic substrates; hydrophilic substrates; 3d-obstacles; collagen film patterning; film-internal cohesion forces; adhesion forces; multifunctional substrate surfaces.

Biographical notes:

Karina Ambrock graduated from the Department of Physics & Astronomy and the University of Applied Science (Gelsenkirchen, Germany) with a Master of Science (Molecular Biology) in 2016. She is now a PhD student with the Münster Electrochemical Energy Technology (MEET) Institute (Germany).

Bernd Grohe is a Senior Research Associate in the Department of Chemical and Biochemical Engineering. His fields of interest are in biomineralization, biomimetics and in the area of chemistry & physics of surfaces.

Silvia Mittler is a Professor in the Department of Physics and Astronomy. Her fields of expertise are the photonics of surfaces & interfaces and coatings & thin films.

1 Introduction

The major structural protein in mammals is collagen (Nimni, 1988; Shoulders and Raines, 2009). The protein exists in several types, whereas the type I is the most abundant form found in e.g. bone, cornea, dermis and tendon (Nimni, 1988; Shoulders and Raines, 2009). Individual type I collagen molecules are composed of three left-handed helical polypeptide chains, which form a right-handed triple-helical structure. This structure is stabilized by hydrogen bonds and the resulting trimeric collagen molecule (so-called tropocollagen) is ~300 nm long and 1.5 nm in diameter (Nimni, 1988; Hulmes, 1992; Hulmes, 2002).

Tropocollagen molecules aggregate in a staggered fashion and form (micro) fibrils (Nimni, 1988). In further steps, bundles of these fibrils form collagen fibers. Thereby, hydrophobic interactions between non-polar regions of adjacent molecules are governing collagen fibril formation (fibrillogenesis) (Cassel, 1966; Cooper, 1970). However, fibrillogenesis is also driven by hydrogen bonding between polar residues (Leikin et al., 1995). In addition, the overall processes can be further controlled by varying the pH, the nature and the concentration of added salts, as well as by adding molecules such as propanol and phosphate (Usha et al., 2006; Li et al., 2009; Ambrock et al., 2018), which enhance the inner cohesion of collagen molecules (Usha et al., 2006).

Depending on the tissue and its function, these fibers can form layers of randomly oriented molecules/fibrils as in woven (immature) bone or dermis (Gross and Schmitt, 1948; Draughn and An, 2000; Currey, 2002), they can show arrangements of high orientation in a single direction

(e.g. in tendon (Squier and Bausch, 1984)) or they may be present as individual layers of highly oriented fibers angled to each other as found in mature bone or cornea (Draughn and An, 2000; Currey, 2002; Meek, 2009). These differences in protein and structure orientation provide the appropriate mechanical properties for the specific tissue (Purslow et al., 1998). Based on these findings, various approaches have shown that collagen can be successfully incorporated into artificial constructs. For example, collagen-rich tissue is chemically modified and used as valve replacements in humans (Meena et al., 1999). Likewise, animal collagen can be extracted, processed, and used for a variety of applications, including wound dressings, cornea/lip augmentation, drug delivery, coating of implants for cell growth enhancement, and many other purposes (Meena et al., 1999; Rammelt et al., 2004; Cai et al., 2014; Niinomi et al., 2014; Corobea et al., 2015; Ghosh et al., 2016). However, despite these successful applications in medicine, mimicking a natural fiber arrangement and orientation as well as supramolecular assemblies in relative large size (10-100 cm²) coatings of thin films are still a major challenge. The reason for that is that all fabricated films and other products/implants need to mimic the supramolecular assemblies they will be replacing in the tissues.

Of course, in recent years various approaches have been developed to produce films or scaffolds that meet the conditions for biomedical applications. Collagen alignment in films is accomplished by magnetic or electrical fields, the application of stress/strain and the Langmuir-Blodgett/Schaefer technology (Narayanan et al., 2014; Pastorino et al., 2014; Chaubaroux et al., 2015; Sorkio et al., 2015; Nam et al., 2016; Bonfrate et al., 2017). Thick films and membranes are fabricated via micro fluidics, stress/strain, extrusion/compacting (Riching et al., 2014; Banglmaier et al., 2015; Nam et al., 2016), while for scaffolds the fabrication can be based on electro spinning, freeze drying, electrochemical treatment, micro fluidics and ‘crowding’ of collagen (English et al., 2012; Kishore et al., 2012; Saeidi et al., 2012; Younesi et al., 2014; Thomas et al., 2016; Islam et al., 2016; Paten et al., 2016; Ryan et al., 2017).

Using the Langmuir-Blodgett (LB) technology (Petty, 1996) for the deposition of collagen, recently a straightforward and inexpensive method was introduced to fabricate ultra-thin coatings of highly oriented type I collagen films ($\sim 10 \text{ cm}^2$) on glass substrates (Tenboll et al., 2010). It was found that the orientation behaviour of collagen molecules during LB-film deposition is comparable to the behaviour of a particular class of synthetic polymers known as hairy rod polymers (Schwiegk et al., 1992; Mittler-Neher et al., 1992; Wegner, 2003a). Both types of molecules show shape persistence (Schwiegk et al., 1992; Mittler-Neher et al., 1992; Wegner, 2003a; Wegner, 2003b; Tenboll et al., 2010), and indicate a highly oriented and preferential alignment in pull-out direction (proceeding from an “orientation arch”) (Schwiegk et al., 1992; Wegner, 2003a; Tenboll et al., 2010). This “orientation arch” develops on the trough during collagen film formation and compression, and is aligned perpendicular to the pull-out direction and parallel to the air-water interface (Tenboll et al., 2010). Besides single coatings, multiple depositions, as well as a deposition procedure in which the substrate was rotated by 90° between two consecutive collagen deposition steps, were performed (Tenboll et al., 2010). This shows that films for wound healing, implant coatings and, in the case of orthogonally aligned collagen layers, the mimicking of the cornea structure are possible. Fabrication of such ultra-thin and highly oriented films is, to the best of our knowledge, not possible using any other method (incl. the Langmuir Schaefer deposition (Sorkio et al., 2015)).

In addition, the dimension and shape of a substrate must be chosen carefully, since the flow conditions of collagen on the LB-trough are imposed by the substrate's shape and its pull-out direction (Nahar et al, 2013).

Recent studies have shown that collagen transfer is possible on both, hydrophilic and hydrophobic surfaces, although most stable films were achieved with freshly prepared collagen solutions, n-propanol as a stabilizer and coating on hydrophobic surface. However, when n-

propanol was replaced by phosphate ions as stabilizer most stable films were produced using hydrophilic substrates (Ambrock et al., 2018).

The objective of the present study is to investigate the effect of physicochemical (hydrophilic/hydrophobic) patterns and 3D-mechanical barriers (located on substrate surfaces) on the collagen flow during LB transfer. This study is virtually a pre-study for collagen coatings on implants with irregular shapes and the fabrication of freestanding collagen films. For this purpose, the cohesion of the forming coating is examined by analyzing the collagen flow from the air-water interface onto the substrate as it encounters an obstacle on the substrate. Although we are using an indirect route instead of direct LB transfer of collagen onto implants (or testing freestanding films), this method provides a first insight into the disturbed film formation and the feasibility (sufficient cohesion, adhesion) of such coatings using a fast, non-toxic and cost-effective process, without wasting valuable implant material.

A second part of the present work deals with the fabrication of substrates each individually patterned to exhibit multiple different physicochemical surfaces (i.e. three equal-sized sections: hydrophilic, hydrophobic, collagen coated). Such experimental substrates are excellently suited for conducting studies under various surface conditions (all other experimental parameters are constant) in a relatively short time. As these platforms are expected to be stable under super-physiological conditions (e.g., temperatures around 37°C [for two months at least] and higher [60°C for at least 10 min.]), and relatively high salt concentrations (Nahar et al., 2013), applications in engineering, chemistry, biology, and material sciences are conceivable. To test the surface effects on a reaction system we carried out a small series of crystal growth experiments.

2 Materials and Methods

2.1 Collagen solutions and other chemicals

Type I collagen (molecular weight: ~300 kDa) was prepared from rat tail tendons as previously described (Hunter et al., 2001). The collagen material obtained has shown to form a triple-helical structure (tropocollagen) (Baht et al., 2008), which is needed for film formation (Tenboll et al., 2010). For LB transfer, 2 μ M collagen solutions were prepared by dissolving 0.6 mg of collagen in mixtures of 0.9 mL acetic acid (5 mM) and 0.1 mL n-propanol for at least 12 h at 4°C (in motion) (Usha et al., 2004). Using n-propanol effectively stabilizes the protein structure and supports LB film formation without directly interacting with collagen molecules (Usha et al., 2006; Tenboll et al., 2010). A silicone based solution (DISCCOAT 4222; General Chemical Cooperation, Mi, USA) was applied on hydrophilic or hydrophobic substrate surfaces, but also on collagen deposited on such substrate surfaces. The silicone drops (different sizes and arrangement) were, e.g., used to investigate flow dynamics of collagen on the different surfaces during collagen deposition.

2.2 Circular dichroism (CD) spectrometry

The prepared collagen solutions were diluted (0.3 mg collagen/mL) using 5 mM acidic acid and then incubated for 2 h at 20 °C. Samples of each solution were transferred to a 1 mm path length quartz cuvette and the ellipticity measured from 185 to 260 nm using a J810 spectropolarimeter (Jasco; Easton, MD, USA) at 20 °C; the temperatures were maintained by a Peltier system (Jasco, PTC 4235). Spectra were also obtained at 60 °C (above the denaturation temperature). For analysis of CD data, relevant literature was consulted (Usha et al., 2006; Greenfield, 2006).

2.3 Preparation of hydrophilic and hydrophobic glass substrates for LB transfer

For hydrophilic glass surfaces and as preconditioning for hydrophobic substrates, glass slides (microscope slides, Bio Nuclear Diagnostics Inc., Toronto, ON, Canada) were thoroughly cleaned by sonication in acetone and Milli-Q water ($\rho \geq 18 \text{ M}\Omega\cdot\text{cm}$, Millipore) for 5 min, respectively. After each step, the substrates were rinsed five times with Milli-Q water. The slides were then immersed in a solution of concentrated H_2SO_4 and H_2O_2 (Piranha: 4:1 [97% H_2SO_4]: [30% H_2O_2]; both Sigma Aldrich) overnight to create $-\text{OH}$ groups on the substrate surface, then rinsed with copious amounts of Milli-Q water, and dried with N_2 .

For hydrophobic glass substrates, glass slides were first preconditioned as described above. The resulting $-\text{OH}$ groups on the glass surfaces are essential for the silanization of substrates. To generate hydrophobic glass surfaces, a 10 mM OTS solution (97%, Sigma-Aldrich) in anhydrous toluene was prepared. Since OTS is moisture sensitive the solution was always prepared under a N_2 /dry atmosphere (glovebox) and used immediately. In the glovebox, the preconditioned glass substrates were then immersed in OTS for 6 h to perform OTS self-assembly, followed by a rinsing step with toluene and ethanol, and drying with N_2 . All chemicals were used without further purification.

2.4 Langmuir-Blodgett (LB) technique

For LB transfer of collagen, substrates were immersed nearly completely (2/3) in the Milli-Q water subphase ($\sim 1/3$ of the substrate length was not immersed but used for mounting). Using a Hamilton syringe, 2 μM collagen solution was applied dropwise to the entire surface of the aqueous subphase in the LB trough (KSV Instruments LTD Model KSV3000-2 LB). Following a 20-min waiting period to allow for the volatile solvent to evaporate the barriers were allowed to compress to ~ 5 mN/m at a speed of 5 mm/min (at 25°C; for details see Tenboll et al., 2010; Ambrock et al., 2018). For LB film transfer, the substrate was then pulled out of the water subphase through the collagen

LB film with the KSV film lift at a speed of 5 mm/min. For collagen deposition onto a further sample, the trough was thoroughly cleaned, refilled with Milli-Q water, and the new substrate mounted nearly completely immersed in the aqueous subphase, before collagen was re-applied and the fabrication process repeated. Films on the air-water interface are referred to as Langmuir films, whereas films transferred on a substrate are called Langmuir-Blodgett films. Within this paper we call both kinds of films LB-films.

2.5 Surface patterning

For patterning of substrate surfaces, silicone drops (cross section: 3-6 mm [or larger, see Fig. 3], thickness ~ 0.2 mm; measured via a digital caliper) were placed either on Piranha-cleaned (hydrophilic), on Piranha-cleaned and then OTS-treated (hydrophobic), or on collagen coated substrate surfaces. The dried silicone buttons were removed to receive a hydrophilic/hydrophobic surface pattern or they were left on the substrate to achieve a button pattern on a hydrophilic and/or hydrophobic surface for further use. For each combination, at least five substrates were fabricated.

2.6 Contact angle measurements

Contact angle measurements (Goniometer NRL Model 100-00, Ramé-Hart, Montréal) were carried out on different substrate surfaces and coatings to characterize their hydrophilic/hydrophobic character. Measurements were taken at least 3 times per sample (in a specific surface area). A strong hydrophilicity shows small contact angles ($\theta < 2^\circ$), whereas hydrophobic surfaces exhibit larger contact angles ($\theta > 100^\circ$).

2.7 Optical microscopy

For analysis of deposited LB-films and silicone droplets, bright and dark field microscopy (Zeiss Axioskop 2 MAT, Oberkochen, Germany) was carried out. Analysis of crystal growth experiments occurred by bright field microscopy (Zeiss Axiovert 25 CFL, Oberkochen, Germany).

2.8 Scanning electron microscopy (SEM) and Fast Fourier Transform (FFT) analysis

A SEM (LEO 1540XB, Carl Zeiss, Oberkochen, Germany) was used to determine the surface structure of the transferred collagen LB-films. The samples were investigated without additional metal coating at an acceleration voltage of 1 kV and a working distance between 3.5 and 4.0 mm.

FFT (ImageJ, version 1.48v; National Institutes of Health, Bethesda, MD, USA) was used to get insight into the orientation of collagen matrices.

2.9 Barium oxalate hydrate ($BaC_2O_4 \cdot xH_2O$) crystallization

Analytical grade barium chloride dihydrate ($BaCl_2 \cdot 2H_2O$; Sigma), sodium oxalate ($Na_2C_2O_4$; J.T. Baker) and sodium chloride ($NaCl$; Sigma) were used as obtained. Deionized water purified with a Milli-Q water system (Millipore filters) and filtration through a 0.2 μm pore size membrane was used for the preparation of all solutions. To initiate crystallization of barium oxalate hydrate ($BaC_2O_4 \cdot xH_2O$), 0.25-ml aliquots of (i) $[Ba^{2+}] = [C_2O_4^{2-}] = 10$ mM (high supersaturation conditions) or (ii) $[Ba^{2+}] = [C_2O_4^{2-}] = 4$ mM and 120 mM $NaCl$ (low supersaturation conditions) were added to substrate surfaces exhibiting various physicochemical characters (treatment see

section 2.2 – 2.4) at 23°C. Oxalate solution was added first to a substrate surface followed by sodium chloride and/or the barium solution. Reactions were carried out for 24 h. Samples were analyzed via optical microscopy.

3 Results and Discussion

The present work investigates the influence of physicochemical patterns and 3D-mechanical barriers (located on the substrate surface) on the formation of highly oriented collagen films fabricated via LB-technology. The aim is to find a way to control the collagen flow during the coating process on glass substrates so that obstacles on these substrates either (a) lead to a defect in the forming collagen layer or (b) alternatively resulting in a defect free film, “ignoring” the obstacles during formation of the collagen coating.

During the film transfer/coating formation, the control of the collagen flow and the alignment through the substrate is guided by the internal cohesion forces, F_{coh} , (hydrophilic-hydrophobic force balance between collagen molecules/aggregates) within the collagen LB-film and the attractive adhesion forces between the collagen film and the hydrophilic or hydrophobic surface of the substrate; F_{adh} . If the cohesive forces (F_{coh}) are disturbed and the adhesion forces (F_{adh}) are strong enough, a film fragmentation can take place in which the individual film fragments show adhesion. However, if the obstacles on a substrate do not overcome F_{coh} then the forming film will ignore the obstacles and, e.g., stretch over “irregularities”.

Recently, Ambrock et al. (2018) have reported a stronger adhesion of LB-collagen films to hydrophobic than to hydrophilic substrates, which implies that $F_{\text{adh,phobic}} > F_{\text{adh,philic}}$. This finding is supported by the fact that collagen can be spread on the air-water interface (Tenboll et al., 2010; Nahar et al., 2013; Ambrock et al., 2018), and observations that LB transfer of amphiphilic fatty

acids is possible only with the hydrophilic side of the LB film to a hydrophilic substrate and the hydrophobic side to a hydrophobic substrate (Ulman, 1991). Consequently, we expect defect formation of coatings to occur when hydrophilic surfaces or phase boundaries (hydrophilic/hydrophobic) are present rather than hydrophobic surfaces. It is assumed, however, that the strongest impact on collagen coating formation will come from 3D-objects that are located on substrate surfaces.

3.1 Confirming triple-helical collagen (Tropocollagen) in solution and LB-area-pressure isotherm

For manufacturing highly oriented collagen films and coatings, it is essential that triple-helical structured collagen (tropocollagen) is present in collagen solutions (Tenboll et al., 2010). To this end, CD spectra of the prepared solutions were determined at 20°C and 60°C, and the results compared to CD spectra reported previously (Usha et al., 2006; Greenfield, 2006). The measurements show (Fig. 1a) that the spectra (at 20°C) are consistent with a triple-helical type I collagen structure without fibrillar components (Greenfield, 2006), and thus are suitable for testing their efficiency in film formation. As expected, the collagen solutions treated at 60°C indicated denatured collagen (Fig. 1a; (Greenfield, 2006)). Bentz et al. (1978) have shown that denaturation of dispersed collagen sets in slightly above 37°C, which means that the triple-helical structure is stable up to a temperature $\sim 37^\circ\text{C}$ and that those films should be transferable.

Collagen solutions (400 μL ; 2 μM) were spread onto the air-water interphase of the LB trough and films compressed up to the minimal trough area. A maximum lateral pressure of ~ 6.5 mN/m and no phase transitions were determined (Fig. 1b), characteristics also observed in previous studies for these films (Tenboll et al., 2010; Nahar et al., 2013; Ambrock et al., 2018). Transfer was performed at $\sim 3/4$ of the max. pressure: ~ 5 mN/m.

3.2 Substrate patterning on substrate surfaces and their control of collagen flow

Several substrates were fabricated using a sequence of manufacturing steps that can be varied for each sample (for details on sample fabrication steps, see also Table 1). First, for a set of controls, glass substrates (Glass) were treated with Piranha (P) to generate a highly hydrophilic surface. Thereafter, a subset of these substrates were either coated with collagen (C) or further treated with OTS to create hydrophobic conditions. Also some of the OTS treated samples were collagen coated. These sample combinations, the Glass-P and Glass-P-OTS as well as the substrates Glass-P-C and Glass-P-OTS-C were all fabricated without further patterning. The contact angles for all sample types can be found in Table 1, sorted by their physicochemical character under the hydrophobic (Glass-P-OTS) or the hydrophilic (Glass-P) platform.

As expected, collagen transfer to the two types of control substrates (hydrophilic: Glass-P; hydrophobic: Glass-P-OTS) resulted in defect free and highly oriented collagen coatings (Tenboll et al., 2010; Ambrock et al., 2018).

3.2.1 Hydrophilic/hydrophobic patterning of substrate surfaces and their effects on the change of collagen flow

For the first set of patterned samples, substrates based on the Glass-P (hydrophilic) and the Glass-P-OTS (hydrophobic) type were prepared by placing one or several silicone drops (Si; cross section: 3-6 mm, thickness ~0.2 mm) on the hydrophilic (P) or hydrophobic (OTS) surface and – after drying – removed (SiRe). This procedure leads to the final combinations Glass-P-[Si-SiRe] or Glass-P-OTS-[Si-SiRe] (Note: In the following, when a dried silicon button is removed from a sample surface the designation within the bracket [...] describes the removed material and the removal (SiRe)). The surface characteristics (Table 1) of these manufactured combinations show

that the contact of the silicon drop with the hydrophilic and the hydrophobic surface induces an increase of the hydrophobicity (compare Glass-P with Glass-P-[Si-SiRe]; contact angels change from < 1 [°] to ~ 35.8 [°]) and a decrease of the hydrophobicity (compare Glass-P-OTS with Glass-P-OTS-[Si-SiRe]; contact angels change from ~ 121.5 [°] to ~ 107.6 [°]), respectively. Very hydrophilic surfaces become less hydrophilic and strong hydrophobic surfaces become less hydrophobic, which indicates a slight change (possibly due to contamination) of the respective surface properties caused by the silicone (Dunn, 2016). Collagen deposition on these samples with different but not extreme surface hydrophobicities and hydrophilicities showed no change in collagen flow: collagen covered the patterned substrate surface completely and defect-free. Even large patterns (from application/removal of large silicon droplets) had no effect on the collagen flow (not shown). The inner cohesion force of the film, F_{coh} , is obviously much larger than the difference in the adhesion forces of the both substrate types, $F_{\text{adh,phil-high}} - F_{\text{adh,phil-low}}$ (the high/low hydrophilic substrate) or $F_{\text{adh,phob-high}} - F_{\text{adh,phob-low}}$ (the high/low hydrophobic substrate), and thus not large enough to induce disruption of collagen flow.

3.2.2 Large differences in the hydrophilic/hydrophobic properties of patterning on substrate surfaces and their effects on the change of collagen flow

Therefore, a second set of patterned substrates was fabricated indicating higher differences in surface adhesion forces. To this end, the preparation method was slightly modified by placing a silicone drop on a Piranha treated substrate, subsequently hydrophobized the entire substrate surface (incl. the dry silicon button) with OTS and finally removed the silicone button. The resulting pattern of this substrate type, a hydrophilic spot (Glass-P-[Si-OTS-SiRe]; removed: [Si-OTS-SiRe]) within a hydrophobic environment (Glass-P-OTS), did, however, not show any influence on collagen flow dynamics (not shown). The large difference in hydrophilicity between

the hydrophilic spot (contact angle: ~ 35.7 [°]) and the hydrophobic surrounding (contact angle: ~ 121.5 [°]; see Table 1) or surface adhesion forces $F_{\text{adh,phil,max}} - F_{\text{adh,phob,max}}$ was not sufficient to overcome the film's inner coherence force F_{coh} . Also in this series of samples, patterning by applying and removing large or several small silicone drops (in a row, perpendicular to the pull-out direction) could not divide the collagen flow. In almost all cases the hydrophilic/hydrophobic obstacles were not able to overcome the internal cohesion forces (F_{coh}) of the collagen coating, although some samples indicated locally ripped (not really divided) collagen coatings (Fig. 2).

These disruptions, which are caused by large surface inhomogeneities, are an indication that the control of collagen flow might be possible via a sufficiently large adhesion force difference that overcomes the inner cohesion force of the collagen film. For the film-surface combinations tested, the inner cohesion forces of the compressed collagen LB films are too strong to be overcome by the weaker hydrophilic/hydrophilic or hydrophobic/hydrophobic adhesion forces between the collagen film and the substrate. This force interplay explains why small hydrophilic areas surrounded by an overall hydrophobic surface can easily be spanned by a highly cohesive collagen film. Vice versa, the small difference in adhesion forces between the collagen LB film and a hydrophilic or hydrophobic surface allows spanning of small hydrophobic areas within an overall hydrophilic substrate surface. It had been shown by Lieser et al. (1994) that the larger majority of < 0.5 -micrometer large holes in hydrophilic formvar films could be spanned by a lipid monolayer LB-film. These films were stable for a few weeks and could be investigated under vacuum conditions in an electron microscope. The inner cohesion of the lipid film must be responsible for the hole-bridging, since in holes the adhesion forces are zero. Therefore, we suspect, that only large surface areas with a large integrated adhesion force difference leads to some disruption of a highly cohesive collagen film. To test this hypothesis, we fabricated even larger hydrophilic areas (contact angle: ~ 35.7 [°]) surrounded by a hydrophobic environment

(contact angle: ~ 121.5 [°]; see Table 1). However, this modification did not lead to a diversion of collagen. Still the strong inner coherence force in the collagen film dominates the LB-transfer.

In general, the use of physicochemical surface variations involving relatively small adhesion interaction forces and force differences is not sufficient to counteract the inner cohesion of collagen molecules and deflect or disrupt its flow. In comparison to the classic fatty acid case, a real amphiphilic molecule class, where, depending on the LB-side, the adhesion forces can be attractive (hydrophilic surface with hydrophilic head group and hydrophobic surface with hydrophobic alkyl chain) or repulsive (hydrophilic surface with hydrophobic alkyl chain and hydrophobic surface with hydrophilic head group), collagen, not amphiphilic, but with more hydrophobic surface groups than hydrophilic, shows explicitly attractive adhesion forces for both surface types.

3.2.3 3D silicon patterning on substrate surfaces and their effects on the change of collagen flow

Based on the configurations Glass-P and Glass-P-OTS, a set of substrates was prepared with the intention to manipulate the flow dynamics via “mechanical” barriers rather than manipulating the adhesion forces. This was realized by placing small or large silicone drops on the strong hydrophilic (Glass-P; contact angle: < 1 [°], Table 1) or strong hydrophobic (Glass-P-OTS; contact angle: ~ 121.5 [°]) surface, respectively, and leave the dried buttons (cross section: 3-6 mm or much larger; thickness ~ 0.2 mm) on the substrate during collagen deposition. Following deposition of collagen on samples with small silicone drops, analysis showed that the produced films cover the entire sample and that these films are either intact or show only minor defects (with no recognizable trend). Therefore, a reproducible flow control of collagen is not possible, although the small buttons appear to have a stronger effect on the flow dynamics than the concept of changing adhesion forces. However, if instead large silicone drops or several small drops (in a

row, perpendicular to the pull-out direction) are applied to the substrate (Fig. 3), most of the experiments lead to a deflection of the collagen flow (Fig. 3a,c,d). For all other ‘large-drop-experiments’ collagen covered the entire sample, incl. the silicon button(s) (Fig 3b). Some experiments showed defective collagen films (Fig. 4b), whether collagen was deflected or not.

Using SEM (Fig. 4) in combination with a Fast Fourier Transform (FFT) analysis, we found that all transferred and large button-deflected films had developed oriented collagen matrices (molecules and/or fibrils), regardless if collagen flow could be controlled or not. The molecules and fibrils are aligned to the fibrillar aggregates and parallel (except the “arch”) to the pull-out direction, as previously found for non-deflected films (Tenboll et al., 2010). FFT analysis was performed only in areas indicating no fibrillar aggregates (e.g. top-left of Fig. 4a or bottom-left Fig. 4c). Fig. 5 depicts the FFT analysis image taken from the area below the white arrow in Fig. 4c. It clearly shows a line (frequency domain) perpendicular to the molecule orientation of the film and the pull-out direction. The higher magnification (Fig. 4c) shows details of the collagen matrix; some larger fibrils and fibrillar aggregates are shown as well. The details of the ultra-thin coating clearly indicate the strict alignment and the high orientation of the collagen structure, a feature that cannot be produced with any other method (to the best of our knowledge) over such large areas (not even via the Langmuir-Schaefer method (Sorkio et al., 2015)). The film thicknesses created under the given conditions are estimated to be in the range between 16 – 20 nm (Tenboll et al., 2010), irrespective of whether collagen solutions were applied to hydrophilic or hydrophobic substrates.

The fact that only large “mechanical” barriers can deflect the flow of collagen is an indication that only large-dimensional 3D-obstacles can overcome the strong inner cohesion forces within the compressed film and tear it, therefore, affecting the collagen flow significantly. This aspect is important in cases where, e.g., 3D-implants are to be coated with collagen and the shapes of these implants show details that are similar to the 3D obstacles created here: small mechanical

obstructions are coated, whereas obstructions with sizes of the order of magnitude of the object itself might lead to interrupted flow and poor coating. Rough and smooth implant surfaces, as well as sub-mm sized screw threads (e.g. of tooth implants) should, therefore, be LB-coatable with oriented collagen and identical quality. However, the details of how threads or other 3D objects are coated need to be investigated in the future.

Assuming that a higher level of hydrophilicity in the collagen "raw material" could decrease the strong inner cohesion (reducing hydrophobic/hydrophobic interactions, a phenomenon recently reported for aged collagen "raw material"; Ambrock et al., 2018), aged collagen solution (stored for 975 days in a freezer at -18°C) was tested for its suitability to control collagen flow conditions in the presence of "mechanical" 3D barriers during coating. However, these films form only locally on the substrate and/or they are pervaded by fissures and other flaws (not shown). The inner cohesion of these 2.5 year aged materials is obviously too much compromised to maintain film formation conditions. More systematic work on less aged material is necessary to tune the inner cohesion forces accordingly. Further control of film formation should be carried out by means of large mechanical barriers, in particular with varying shapes and heights, both in the classic planar substrate fashion and also with real 3D-substrates. The use of other than silicone materials to create the barriers is conceivable. In addition, the sample geometry, its pull-out direction and speed can be varied to additionally affect the flow of collagen and its patterning (Tenboll et al., 2010; Nahar et al., 2013). Using these techniques allows – in part – controlling the flow-dynamic of collagen and thus the patterning of substrate surfaces with collagen films, which is an important parameter to tailor application-specific films and coatings.

An interesting and surprising aspect of our findings is the fact that defects partly led to loosened large-area collagen films. This is an indication that a future fabrication of freestanding, ultra-thin and highly oriented films appears to be possible. Films like this, not bonded to a stiff substrate, can be used (after sterilization) for, e.g., wound dressings exhibiting a controlled collagen

orientation in different layers to mimic the compliance (Young's modulus) of skin or as artificial cornea.

3.3 Substrate patterning by selective removal of LB-transferred collagen and possible applications of such patterned substrates

3.3.1 Fabrication of substrates with multiple physicochemical surfaces

An alternative route to 'flow-patterning' is to pattern collagen-coated substrates in a 2-step-process: first the substrate is coated via the LB-transfer and then parts of the deposited collagen film are removed to create the patterning. To this end, hydrophobic (Glass-P-OTS) or hydrophilic (Glass-P) substrates were coated with collagen. The patterning was performed by placing one or more silicone drops on top of the collagen-coated substrates and, after drying, removing the silicone buttons. The following combinations were created: Glass-P-[C-Si-SiRe] and Glass-P-OTS-[C-Si-SiRe] (note: removing a silicon drop results also in the remove of collagen). Such samples (see Fig. 6) exhibit either hydrophilic (contact angle: ~ 36.0 [°]) or hydrophobic (contact angle: ~ 107.1 [°]) spots within a collagen environment indicating contact angles of (Glass-P-C) ~ 52.7 [°] and (Glass-P-OTS-C) ~ 54.8 [°], respectively (see also Table 1).

Similar substrates were fabricated if the combinations Glass-P-[Si-C-SiRe] and Glass-P-OTS-[Si-C-SiRe] were used, whereas the part within the brackets [...] was removed with the silicon button. Contact angles of the created spots changed only marginally compared to the former data of the substrates: ~ 35.4 [°] for the hydrophilic and 107.8 [°] for the hydrophobic surface, respectively. Contact angles of the collagen environment surrounding the spots do not vary.

Also possible are combinations such as Glass-P-C-Si or Glass-P-OTS-C-Si, where collagen is coated but the dried silicone buttons are not removed. Here very hydrophobic islands (Glass-P-C-

Si; contact angle: ~ 140.7 [°] or Glass-P-OTS-C-Si; contact angle: ~ 146.7 [°]; see Table 1) in a collagen environment (contact angle: ~ 52 - 54 [°]) are created.

3.3.2 Application of substrates with multiple physicochemical surfaces side by side: crystallization of barium oxalate hydrate

These patterned substrates, each having several surfaces with different physicochemical characters, are excellently suited to perform experiments side by side by implementing these various kinds of surfaces under otherwise identical conditions. Two examples: (a) Cell response to different topographies (Ertorer et al., 2013) and to hydrophilic/hydrophobic surfaces (Weiss and Blumenson, 1967) can be examined in parallel to each other. (b) It is expected that crystallization and aggregation processes will produce different nucleation rates, crystal morphologies and aggregates, using these different substrate surfaces side by side (see e.g. Grohe et al., 2011, 2012; Sethmann et al., 2014; Grohe, 2017).

A preliminary proof-of-concept-study on the crystallization of pyrotechnically relevant barium oxalate hydrate was performed (see Fig. 7). The optical micrographs (Fig. 7) show that in cases of low supersaturation ($[\text{Ba}^{2+}] = [\text{C}_2\text{O}_4^{2-}] = 4$ mM; 120 mM NaCl), needle-like (~ 0.2 - 2 mm long) crystals grew on hydrophilic (up to 4-5 crystals/unit area were counted) and on collagen surfaces (1-2 crystals/unit area), but not on hydrophobic substrate surface. The high supersaturation ($[\text{Ba}^{2+}] = [\text{C}_2\text{O}_4^{2-}] = 10$ mM), which causes a higher nucleation rate, formed small irregular shaped crystals (diameter ~ 1 – 15 μm) and aggregates in large quantities at the hydrophilic surface, in a smaller number on collagen coatings and again fewer of those crystals at the hydrophobic surfaces. These results are in excellent agreement with previous studies on BaC_2O_4 using individual ‘substrates’ and varying reaction conditions (Raj et al., 2008; Ding et al., 2013). In addition, comparing these outcomes with the contact angles of the respective surfaces (see Table 1) shows an excellent

agreement of high precipitation rates with high hydrophilicities. In other words, the presence of a hydrophilic surface provides (in contrast to hydrophobic surfaces) a higher number of nucleation sites and, therefore, results in a higher number of formed crystals.

The crystallization experiment described here is a simple example, for the versatile use of patterned collagen substrates. The execution of experiments in a short time is another advantage when using these multi-platform substrates. Applications in chemistry and biochemistry, engineering and biotechnology, material sciences and mineralogy as well as for physical and metallurgical tasks are conceivable. Specific examples are, besides the examination of crystallization processes, the study of bacterial behaviour (incl. population growth) under different conditions, the testing of different constructs for specific (stem)cell work and scaffolds, or the study of adsorption/desorption processes. Since these substrates are relatively insensitive under physiological and super-physiological conditions (e.g., temperatures: 37-55 ° C, relatively high salt concentrations) (Li et al., 2009; Nahar et al., 2013), it is expected that experiments can run for a relatively long time under these conditions. In addition, additives such as dyes and proteins can be present during experiments as they are not affecting the quality of these substrates (Baht et al., 2008).

4 Conclusions

We have studied the effects of physicochemical (hydrophilic/hydrophobic) patterns and 3D-mechanical barriers present on substrate surfaces on the dynamics of collagen flow during LB-film deposition for highly oriented coatings.

1. Only large 3D obstacles or a row of several small 3D obstacles (perpendicular to pull-out the direction) can deflect the flow of collagen effectively.
2. Single small buttons or just hydrophilic areas in a hydrophobic environment (or vice versa) are easily spanned by the highly cohesive collagen LB-film.
3. The inner cohesion forces of a collagen LB-film are larger than the attractive adhesion forces between the collagen film and the hydrophilic or hydrophobic surface during LB-transfer: $F_{\text{coh}} > F_{\text{adh}}$.
4. This coating behaviour is important (e.g. for biocompatibility reasons) if 3D-implants, such as screw-threaded dental implants, are to be coated with oriented collagen. Such objects, which have topographical features of small size, should be readily and uniformly coatable with highly oriented collagen using the LB technique - no deflection of collagen flow is expected at/near at these small features, and therefore no rupture of the coating.
5. The fabrication of freestanding films should be possible.
6. Patterned samples each having multiple surfaces with different physicochemical characters were prepared by an alternative approach, not controlling the flow on the trough, but simply removing deposited collagen successfully from the sample in a patterned fashion. These substrates are excellently suited to perform experiments on one substrate with different surfaces side by side under otherwise identical conditions.
7. A simple example of a surface-nucleation-controlled crystallization process was discussed. The execution of experiments in a short time is an advantage when using these multi-platform substrates.

Acknowledgements

The authors thank the Nanofabrication Facility (Faculty of Science, University of Western Ontario [UWO]) for hosting the LB trough and the optical Zeiss Axioskop microscope. The authors thank Todd Simpson (Nanofabrication Facility, Faculty of Science, UWO) for assistance with electron microscopy and Lee-Ann Briere (Bimolecular Interactions and Conformations Facility, Department of Biochemistry, UWO) for help in CD spectroscopy. Harvey Goldberg (School of Dentistry, UWO) is gratefully acknowledged for providing valuable reagents and Brian Davis (Department of Physics & Astronomy, UWO) for carefully reading the manuscript. These studies were supported by the Natural Sciences and Engineering Research Council of Canada.

References

- Ambrock, K., Grohe, B. and Mittler, S. (2018) ‘Controlling the hydrophilicity and cohesion during deposition of highly oriented type I collagen films: An approach for biomedical applications’, *Thin Solid Films*, Vol. 656, pp.75-82.
- Baht, G.S., Hunter, G.K. and Goldberg, H.A. (2008) ‘Bone sialoprotein-collagen interaction promotes hydroxyapatite nucleation’, *Matrix Biology*, Vol. 27, No. 7, pp.600-608.
- Banglmaier, R.F., Sander, E.A. and Van de Vord, P.J. (2015) ‘Induction and quantification of collagen fiber alignment in a three-dimensional hydroxyapatite-collagen composite scaffold’, *Acta Biomaterialia*, Vol. 17, pp.26-35.

- Bentz, H., Bachinger, H.P., Glanville, R., and Kuhn, K. (1978) 'Physical Evidence for the Assembly of a-Chains and B-Chains of Human Placental Collagen in a Single Triple Helix', *European Journal of Biochemistry*, Vol. 93, No. 2, pp.563-567.
- Bonfrate, V., Manno, D., Serra, A., Salvatore, L., Sannino, A., Buccolieri, A., Serra, T. and Giancane, G. (2017) 'Enhanced electrical conductivity of collagen films through long-range aligned iron oxide nanoparticles', *Journal of Colloid and Interface Science*, Vol. 501, pp.185-191.
- Cai, F., Miyata, C., Huang, X., & Yang, Q. (2014) 'Microstructure, bioactivity and wear resistance of sintered composite Co-Cr-Mo/Bioglass((R)) for medical implant applications', *International Journal of Surface Science and Engineering*, Vol. 8, No. 2-3, pp.264-281.
- Cassel, J.M. (1966) 'Collagen Aggregation Phenomena', *Biopolymers*, Vol. 4, No. 9, pp.989-997.
- Chaubaroux, C., Perrin-Schmitt, F., Senger, B., Vidal, L., Voegel, J.C., Schaaf, P., Haikel, Y., Boulmedias, F., Lavallo, P. and Hemmerle, J. (2015) 'Cell Alignment Driven by Mechanically Induced Collagen Fiber Alignment in Collagen/Alginate Coatings', *Tissue Engineering Part C-Methods*, Vol. 21, No. 9, pp.881-888.
- Cooper, A. (1970) 'Thermodynamic Studies of Assembly in-vitro of Native Collagen Fibrils', *Biochemical Journal*, Vol. 118, No. 3, pp.355-365.

- Corobea, M.S., Albu, M.G., Ion, R., Cimpean, A., Miculescu, F., Antoniac, I.V., Raditoiu, V., Sirbu, I., Stoenescu, M., Voicu, S.I. and Ghica, M.V. (2015) 'Modification of titanium surface with collagen and doxycycline as a new approach in dental implants', *Journal of Adhesion Science and Technology*, Vol. 29, No. 23, pp.2537-2550.
- Currey, J.D. (2002) *Bones: structure and mechanics*, Oxford, Princeton University Press, Princeton, New Jersey.
- Ding, S.S., Lei, M., Xiao, H., Zhang, Y.C., Huang, K., Liang, C., Wang, Y.J., Liu, G., Zhang, R., Fu, X.L., Fan, D.Y., Yang, H.J. and Wang, Y.G. (2013) 'Morphology evolution of barium oxalate hydrate controlled by poly (sodium-4-styrenesulfonate)', *Powder Technology*, Vol. 249, pp.140-145.
- Draughn, R.A. and An, Y.A. (2000) (Eds.) *Mechanical Testing of Bone and Bone-Implant Interface*, CRC Press, Boca Raton, Florida.
- Dunn, B.D. (2016) *Materials and processes: for spacecraft and high reliability applications*, Springer, International Publishing Switzerland.
- English, A., Azeem, A., Gaspar, D.A., Keane, K., Kumar, P., Keeney, M., Rooney, N., Pandit, A. and Zeugolis, D.I. (2012) 'Preferential cell response to anisotropic electro-spun fibrous scaffolds under tension-free conditions', *Journal of Materials Science-Materials in Medicine*, Vol. 23, No. 1, pp.137-148.

- Ertorer, E., Vasefi, F., Keshwah, J., Najiminaini, M., Halfpap, C., Langbein, U., Carson J.J.L., Hamilton, D.W. and Mittler, S. (2013) 'Large area periodic, systematically changing, multishape nanostructures by laser interference lithography and cell response to these topographies', *Journal of Biomedical Optics*, Vol. 18, No. 3, 035002 (4 March 2013).
- Ghosh, S., Choudhury, D., & Pinguan-Murphy, B. (2016) 'Lubricating ability of albumin and globulin on artificial joint implants: a tribological perspective', *International Journal of Surface Science and Engineering*, Vol. 10, No. 2, pp.193-206.
- Greenfield, N.J. (2006) 'Using circular dichroism collected as a function of temperature to determine the thermodynamics of protein unfolding and binding interactions', *Nature Protocols*, Vol. 1, No.6, pp.2527-2535.
- Grohe, B., Chan, B.P.H., Sørensen, E.S., Lajoie, G., Goldberg, H.A. and Hunter, G.K. (2011) 'Cooperation of phosphates and carboxylates controls calcium oxalate crystallization in ultrafiltered urine', *Urological Research*, Vol. 39, pp.327-338.
- Grohe, B., Hug, S., Langdon, A., Jalkanen, J., Rogers, K.A., Goldberg, H.A., Karttunen, M. and Hunter, G.K. (2012) 'Mimicking the Biomolecular Control of Calcium Oxalate Monohydrate Crystal Growth: Effect of Contiguous Glutamic Acids', *Langmuir*, Vol. 28, No. 33, pp.12182-12190.
- Grohe, B. (2017) 'Synthetic peptides derived from salivary proteins and the control of surface charge densities of dental surfaces improve the inhibition of dental calculus formation',

Materials Science and Engineering C-Materials for Biological Application, Vol. 77, pp.58-68.

Gross, J. and Schmitt, F.O. (1948) 'The structure of human skin collagen as studied with the electron microscope', *Journal of Experimental Medicine*, Vol. 88, pp.555–567.

Hulmes, D.J.S. (1992) 'The collagen superfamily - diverse structures and assemblies', *Essays in Biochemistry*, Vol. 27, pp. 49-67.

Hulmes, D.J.S. (2002) 'Building collagen molecules, fibrils, and suprafibrillar structures', *Journal of Structural Biology*, Vol. 137, No. 1-2, pp.2-10.

Hunter, G.K., Poitras, M.S., Underhill, T.M., Grynbas, M.D., & Goldberg, H.A. (2001) 'Induction of collagen mineralization by a bone sialoprotein-decorin chimeric protein', *Journal of Biomedical Materials Research*, Vol. 55, No. 4, pp.496-502.

Islam, A., Younesi, M., Mbimba, T. and Akkus, O. (2016) 'Collagen Substrate Stiffness Anisotropy Affects Cellular Elongation, Nuclear Shape, and Stem Cell Fate toward Anisotropic Tissue Lineage', *Advanced Healthcare Materials*, Vol. 5, No. 17, pp.2237-2247.

Kishore, V., Uquillas, J.A., Dubikovsky, A., Alshehabat, M.A., Snyder, P.W., Breur, G.J. and Akkus, O. (2012) 'In vivo response to electrochemically aligned collagen bioscaffolds', *Journal of Biomedical Materials Research Part B-Applied Biomaterials*, Vol. 100B, No. 2, pp.400-408.

- Leikin, S., Rau, D.C. and Parsegian, V.A. (1995) 'Temperature-Favored Assembly of Collagen Is Driven by Hydrophilic Not Hydrophobic Interactions', *Nature Structural Biology*, Vol. 2, No. 3, pp.205-210.
- Li, Y.P., Asadi, A., Monroe, M.R. and Douglas, E.P. (2009) 'pH effects on collagen fibrillogenesis in vitro: Electrostatic interactions and phosphate binding', *Materials Science & Engineering C-Biomimetic and Supramolecular Systems*, Vol. 29, No. 5, pp.1643-1649.
- Lieser, G., Mittler-Neher, S., Spinke, J. and Knoll, W. (1994) 'Electron-Microscopic Investigations on Freestanding Mixed Lipid Langmuir-Blodgett-Kuhn Monolayers - Phase-Separation and Aging Process', *Biochimica Et Biophysica Acta-Biomembranes*, Vol. 1192, No. 1, pp.14-20.
- Meek, K.M. (2009) 'Corneal collagen—its role in maintaining corneal shape and transparency', *Biophysical Reviews*, Vol. 2009, No. 1, pp.83–93.
- Meena, C., Mengi, S.A. and Deshpande, S.G. (1999) 'Biomedical and industrial applications of collagen', *Proceedings of the Indian Academy of Sciences-Chemical Sciences*, Vol. 111, No. 2, pp.319-329.
- Mittler-Neher, S., Neher, D., Stegeman, G.I., Embs, F.W. and Wegner, G. (1992) 'Polarization Dependent Resonant THG on Langmuir-Blodgett Multilayers of Rod-Like Polysilanes during Annealing', *Chemical Physics*, Vol. 161, No. 1-2, pp.289-297.

- Nahar, Q., Quach, D.M.L., Darvish, B., Goldberg, H.A., Grohe, B. and Mittler, S. (2013) 'Orientation Distribution of Highly Oriented Type I Collagen Deposited on Flat Samples with Different Geometries', *Langmuir*, Vol. 29, No. 22, pp.6680-6686.
- Nam, E., Lee, W.C. and Takeuchi, S. (2016) 'Formation of Highly Aligned Collagen Nanofibers by Continuous Cyclic Stretch of a Collagen Hydrogel Sheet', *Macromolecular Bioscience*, Vol. 16, No. 7, pp.995-1000.
- Narayanan, B., Gilmer, G.H., Tao, J.H., De Yoreo, J.J. and Ciobanu, C.V. (2014) 'Self-Assembly of Collagen on Flat Surfaces: The Interplay of Collagen-Collagen and Collagen-Substrate Interactions', *Langmuir*, Vol. 30, No. 5, pp.1343-1350.
- Niinomi, M., Nakai, M., Hieda, J., Cho, K., Kasuga, T., Hattori, T., et al. (2014) 'A review of surface modification of a novel low modulus beta- type titanium alloy for biomedical applications', *International Journal of Surface Science and Engineering*, Vol. 8, No. 2-3, pp.138-152.
- Nimni, M.E. (1988) (Ed.) *Collagen Vol. I, Biochemistry*, CRC Press, Boca Raton, Florida.
- Pastorino, L., Dellacasa, E., Scaglione, S., Giulianelli, M., Sbrana, F., Vassalli, M. and Ruggiero, C. (2014) 'Oriented collagen nanocoatings for tissue engineering', *Colloids and Surfaces B-Biointerfaces*, Vol. 114, pp.372-378.

- Paten, J.A., Siadatt, S.M., Susilo, M.E., Ismail, E.N., Stoner, J.L., Rothstein, J.P. and Ruberti, J.W. (2016) 'Flow-Induced Crystallization of Collagen: A Potentially Critical Mechanism in Early Tissue Formation', *Acs Nano*, Vol. 10, No. 5, pp.5027-5040.
- Petty, M.C. (1996) *Langmuir-Blodgett films: an introduction*, Cambridge University Press, Cambridge, New York.
- Purslow, P.P., Wess, T.J. and Hukins, D.W.L. (1998) 'Collagen orientation and molecular spacing during creep and stress-relaxation in soft connective tissues', *Journal of Experimental Biology*, Vol. 201, No. 1, pp.135-142.
- Raj, A.M.E., Jayanthi, D.D., Jothy, V.B., Jayachandran, M. and Sanjeeviraja, C. (2008) 'Growth aspects of barium oxalate monohydrate single crystals in gel medium', *Crystal Research and Technology*, Vol. 43, No. 12, pp.1307-1313.
- Rammelt, S., Schulze, E., Bernhardt, R., Hanisch, U., Scharnweber, D., Worch, H., Zwipp, H. and Biewener, A. (2004) 'Coating of titanium implants with type-I collagen', *Journal of Orthopaedic Research*, Vol. 22, No. 5, pp.1025-1034.
- Riching, K.M., Cox, B.L., Salick, M.R., Pehlke, C., Riching, A.S., Ponik, S.M., Bass, B.R., Crone, W.C., Jiang, Y., Weaver, A.M., Eliceiri, K.W. and Keely, P.J. (2014) '3D Collagen Alignment Limits Protrusions to Enhance Breast Cancer Cell Persistence', *Biophysical Journal*, Vol. 107, No. 11, pp.2546-2558.

- Ryan, A. J., Lackington, W. A., Hibbitts, A. J., Matheson, A., Alekseeva, T., Stejskalova, A., Roche, P. and O'Brien, F.J. (2017) 'A Physicochemically Optimized and Neuroconductive Biphasic Nerve Guidance Conduit for Peripheral Nerve Repair', *Advanced Healthcare Materials*, Vol., 6, No. 24, Artn.: 1700954.
- Saeidi, N., Karmelek, K.P., Paten, J.A., Zareian, R., DiMasi, E. and Ruberti, J.W. (2012) 'Molecular crowding of collagen: A pathway to produce highly-organized collagenous structures', *Biomaterials*, Vol. 33, No. 30, pp.7366-7374.
- Schwiegk, S., Vahlenkamp, T., Xu, Y.Z. and Wegner, G. (1992) 'Origin of Orientation Phenomena Observed in Layered Langmuir-Blodgett Structures of Hairy-Rod Polymers', *Macromolecules*, Vol. 25, No. 9, pp.2513-2525.
- Sethmann, I., Grohe, B., & Kleebe, H.J. (2014) 'Replacement of hydroxylapatite by whewellite: implications for kidney-stone formation', *Mineralogical Magazine*, Vol. 78, No. 1, pp.91-100.
- Shoulders, M.D. and Raines, R.T. (2009) 'Collagen Structure and Stability', *Annual Review of Biochemistry*, Vol. 78, pp.929-958.
- Sorkio, A.E., Vuorimaa-Laukkanen, E.P., Hakola, H.M., Liang, H.M., Ujula, T.A., Valle-Delgado, J.J., Osterberg, M., Yliperttula, M.L. and Skottman, H. (2015) 'Biomimetic collagen I and IV double layer Langmuir-Schaefer films as microenvironment for human pluripotent stem cell derived retinal pigment epithelial cells', *Biomaterials*, Vol. 51, pp.257-269.


- Squier, C.A. and Bausch, W.H. (1984) '3-Dimensional Organization of Fibroblasts and Collagen Fibrils in Rat Tail Tendon', *Cell and Tissue Research*, Vol.238, No. 2, pp.319-327.
- Tenboll, A., Darvish, B., Hou, W.M., Duwez, A.S., Dixon, S.J., Goldberg, H.A., Grohe, B. and Mittler, S. (2010) 'Controlled Deposition of Highly Oriented Type I Collagen Mimicking In Vivo Collagen Structures', *Langmuir*, Vol. 26, No. 14, pp.12165-12172.
- Thomas, D., Gaspar, D., Soroushanova, A., Milcovich, G., Spanoudes, K., Mullen, A.M., O'Brien, T., Pandit, A. and Zeugolis, D.I. (2016) 'Scaffold and scaffold-free self-assembled systems in regenerative medicine', *Biotechnology and Bioengineering*, Vol. 113, No. 6, pp.1155-1163.
- Ulman, A. (1991) *An introduction to ultrathin organic films : from Langmuir-Blodgett to self-assembly*, Academic Press, Boston, USA.
- Usha, R., Dhathathreyan, A., Mandal, A.B. and Ramasami, T. (2004) 'Behavior of collagen films in presence of structure modifiers at solid-liquid interface', *Journal of Polymer Science Part B-Polymer Physics*, Vol. 42, No. 21, pp.3859-3865.
- Usha, R., Maheshwari, R., Dhathathreyan, A. and Ramasami, T. (2006) 'Structural influence of mono and polyhydric alcohols on the stabilization of collagen', *Colloids and Surfaces B-Biointerfaces*, Vol. 48, No. 2, pp.101-105.
- Wegner, G. (2003a) 'Nanocomposites of hairy-rod macromolecules: Concepts, constructs, and materials', *Macromolecular Chemistry and Physics*, Vol. 204, No. 2, pp.347-357.






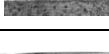
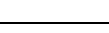





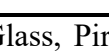
Wegner, G. (2003b) ‘Shape persistence as a concept in the design of macromolecular architectures’, *Macromolecular Symposia*, Vol. 201, pp.1-9.

Weiss, L. and Blumenson, L.E. (1967) ‘Dynamic Adhesion and Separation of Cells in Vitro. 2. Interactions of Cells with Hydrophilic and Hydrophobic Surfaces’, *Journal of Cellular Physiology*, Vol. 70, No. 1, pp.23-32.

Younesi, M., Islam, A., Kishore, V., Anderson, J.M. and Akkus, O. (2014) ‘Tenogenic Induction of Human MSCs by Anisotropically Aligned Collagen Biotextiles’, *Advanced Functional Materials*, Vol. 24, No. 36, pp.5762-5770.

Table 1 Contact angles of differently treated and patterned substrate surfaces. The part within the bracket [...] is removed with an applied, dried and removed silicone drop/button.

Sample Surface *		Contact Angel [°]	Example Image
Glass ^A		≤ 1	
Hydrophobic Platform	Hydrophilic Platform		

Glass-P-OTS ^B		121.54 ± 0.09	
Glass-P-OTS-C ^C		54.84 ± 0.05	
Glass-P-OTS-C-Si ^D		146.70 ± 0.52	
Glass-P-OTS-[C-Si-SiRe] ^E		107.09 ± 0.42	
Glass-P-OTS-[Si-C-SiRe] ^F		107.77 ± 0.33	
Glass-P-OTS-[Si-SiRe] ^G		107.58 ± 0.82	
	Glass-P ^H	< 1	
	Glass-P-C ^I	52.70 ± 0.07	
	Glass-P-C-Si ^J	140.66 ± 0.05	
	Glass-P-[C-Si-SiRe] ^K	36.03 ± 0.89	
	Glass-P-[Si-C-SiRe] ^L	35.39 ± 1.14	
	Glass-P-[Si-SiRe] ^M	35.81 ± 0.47	
	Glass-P-[Si-OTS-SiRe] ^N	35.72 ± 0.23	

Labelling: ^A Glass (as received); ^B Glass, Piranha-cleaned than OTS-treated; ^C Glass, Piranha-cleaned, OTS-treated than Collagen transferred; ^D Glass, Piranha-cleaned, OTS-treated, Collagen transferred than Silicone drop applied; ^E Glass, Piranha-cleaned, OTS-treated, Collagen transferred, Silicone drop applied than Silicone button removed; ^F Glass, Piranha-cleaned, OTS-treated, Silicone drop applied, Collagen transferred, than Silicone button removed; ^G Glass, Piranha-cleaned, OTS-treated, Silicone drop applied than Silicone button removed; ^H Glass, Piranha-cleaned; ^I Glass, Piranha-cleaned than Collagen transferred; ^J Glass, Piranha-cleaned, Collagen transferred than Silicone drop applied; ^K Glass, Piranha-cleaned, Collagen transferred, Silicone drop applied than Silicone button removed; ^L Glass, Piranha-cleaned, Silicone drop applied, Collagen transferred, than Silicone button removed; ^M Glass, Piranha-cleaned, Silicone drop applied than Silicone button removed; ^N Glass, Piranha-cleaned, Silicone drop applied, OTS-treated than Silicone button removed. * If a silicone button is removed the part within the bracket [...] is removed with this drop/button. Contact angles were measured in areas where a silicone drop was previously placed and then removed or directly at the substrate surface/silicone button.

Figure 1 CD spectra and LB surface pressure – trough area isotherm. (a) CD spectra of collagen type I dissolved in acetic acid/n-propanol and measured at 20°C and at 60°C. (b) Surface pressure – trough area isotherm of spread collagen solution.

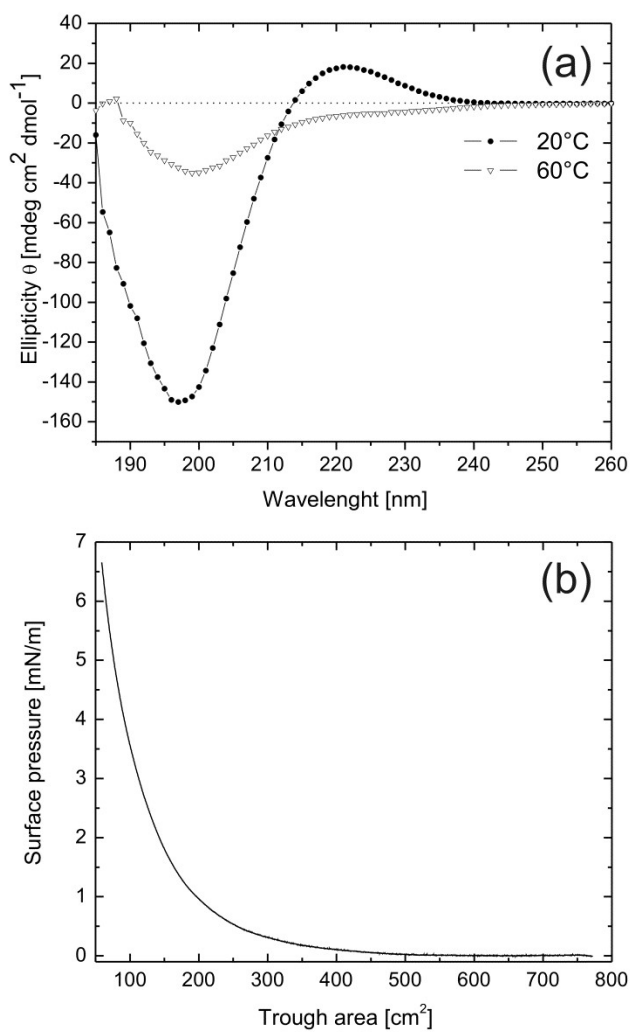


Figure 2 Optical micrograph of a rupture in a collagen film deposited on a (a) hydrophilic (Glass-P) substrate (patterned by applying and removing several small silicone drops), dark field image; white arrows: boundary between collagen coated and uncoated sections of the sample. The small

white dots are artefacts. (b) Schematic drawing of the rupture shown in (a); for clarification purposes. Scale bar in (a): 200 μm .

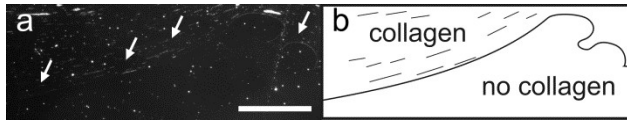


Figure 3 Optical microscopy (bright field images) of deposited collagen structures on (a) hydrophilic (Glass-P) or (b) hydrophobic (Glass-P-OTS) substrate surfaces, onto which (a) a large or (b) a row of smaller silicone drops were applied and the dried button(s) then removed (Glass-

P-[Si-SiRe] or Glass-P-OTS-[Si-SiRe]) before collagen was deposited. (a) Deflection of collagen flow by a large button; (b) collagen was flown over a silicon button. The small black dots in (a,b) are artifacts. If deflection of collagen flow occurred, the patterns shown in sketches (c) and (d) were created. The dotted (thicker) lines represent the silicone button(s) shape, whereas the solid lines represent the deflected collagen fiber orientation. Scale bars: (a): 100 μm , (b) 200 μm .

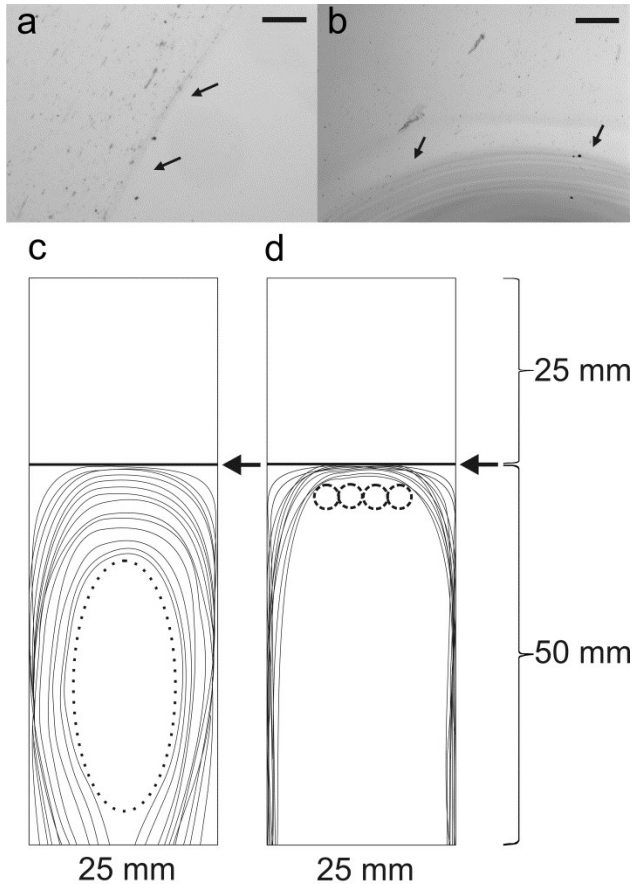


Figure 4 SEM micrographs of collagen films transferred (a) to a hydrophilic and (b,c) to hydrophobic substrates. The overview section shown in (a) is located to the left in the lower third of the sample. Panel (b) shows a defective area (located right, near bottom). (c) The higher

magnification exhibits fibrils and fibrillar aggregates embedded in the collagen matrix. Black arrow: pull-out direction. Scale bars: a: 100 μm ; b: 5 μm ; c: 3 μm .

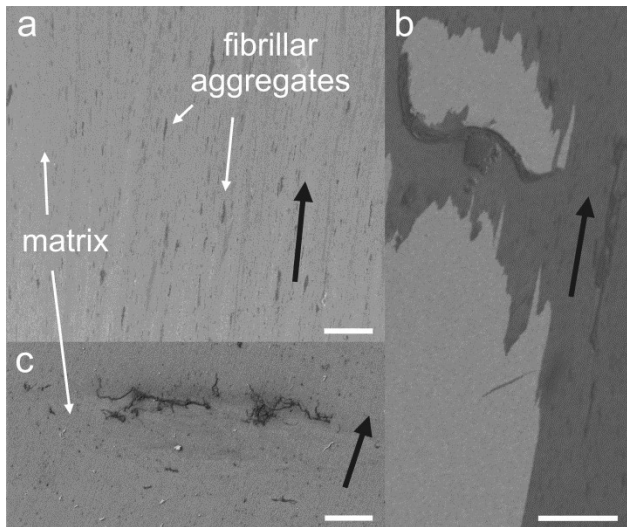


Figure 5 FFT analysis of the collagen matrix depicted in the SEM image of Fig.4c below the white arrow. Clearly a white line (frequency domain) perpendicular to the preferential molecule orientation of the film and the pull-out direction (black arrow in Fig.4c) is shown.

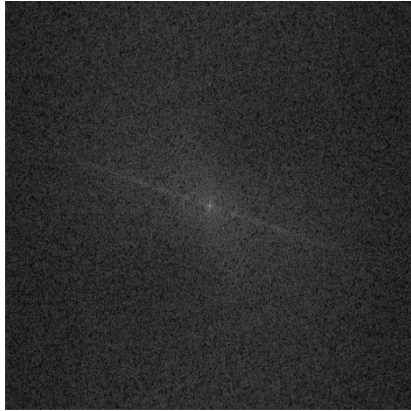


Figure 6 Optical micrographs of patterned (apply/remove silicone) substrate surfaces. (a) A hydrophilic (Glass-P) substrate was collagen coated, then small or large silicone drops were applied and the dried button(s) removed (Glass-P-[C-Si-SiRe]. (b) Same as (a) but OTS treated before collagen was deposited (Glass-P-OTS-[C-Si-SiRe]. (c) At a hydrophilic (Glass-P) substrate

surface small or large silicone drops were applied, then the substrate coated with collagen and the button(s) removed (Glass-P-[Si-C-SiRe]). (d) Same as (c) but OTS treated before the silicone drops were applied (Glass-P-OTS-[Si-C-SiRe]). The black and white arrows show the phase boundaries between collagen and a hydrophilic/hydrophobic substrate surface, created by removing the silicon buttons (incl. collagen). (a,b,d) are bright field images; (c) is a dark field image. Scale bars: (a),(c): 400 μm ; (b),(d): 200 μm .

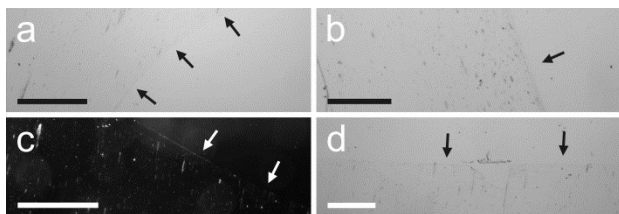


Figure 7 Effects of hydrophilic, hydrophobic and collagen surfaces on barium oxalate formation under two different supersaturation conditions. (a-c) crystal growth using the low supersaturation and hydrophilic substrates (see text and sec. 2.8.); (a) magnified section of crystal shown in (b); (c) needle-shaped crystal, most common shape found under these conditions. (d-h) crystal growth

under high supersaturation conditions (see also sec. 2.8.); high nucleation rates are observed on (d) hydrophilic surfaces, less crystals nucleate on (e) collagen coated surfaces (here hydrophilic substrate) and only a few crystals form on (f) hydrophobic substrates. (g) Collagen coated hydrophobic substrate ((h) magnified section) with a disrupted coating, crystals grew exclusively on collagen. Scale bars – (a),(d),(f),(h): 100 μm ; (b),(e),(g): 500 μm ; (c): 50 μm .

